Polymer Chemistry

COMMUNICATION

Cite this: *Polym. Chem.*, 2016, **7**, 5347

Received 29th July 2016,
Accepted 6th August 2016

DOI: 10.1039/c6py01319h

www.rsc.org/polymers

Surface-initiated polymerization-induced self-assembly of bimodal polymer-grafted silica nanoparticles towards hybrid assemblies in one step†

Yang Zheng, Yucheng Huang, Zaid M. Abbas and Brian C. Benicewicz*

The first case of surface-initiated polymerization-induced self-assembly (SI-PISA) by polymerizing benzyl methacrylate from SiO_2-*g*-(PHEMA, CPDB) in methanol is reported. Hybrid nano-objects with string-shaped morphologies were obtained in one step.

Polymerization-induced self-assembly of block copolymers (PISA) has drawn considerable attention over the past ten years since the seminal reports by Pan *et al.*[1,2] Compared with the traditional method of preparing block copolymer assemblies, PISA has the advantages of a one-step reaction and relatively high solids content (20–50% w/w).[3,4] Typically, a soluble homopolymer is synthesized and chain-extended with a second monomer that when polymerized, becomes insoluble and drives *in situ* self-assembly to form stable nano-objects. A wide range of nanostructures have been observed, including spherical micelles, worms, octopi structures, jellyfish structures and vesicles.[5] A variety of controlled radical polymerization methods (NMP,[6] ATRP,[7] RAFT[8–10]) have been used for PISA with RAFT being the most widely studied. Despite great versatility of PISA in terms of polymerization techniques, reaction solvent and monomer selection, as far as we know, very few attempts have been made to prepare hybrid assemblies that are composed of polymers and inorganic nanoparticles.[11] Recently, Tan *et al.* and Armes *et al.* successfully encapsulated silica nanoparticles within vesicles during PISA synthesis.[12,13] However, there was no control over the assembly of the encapsulated nanoparticles. Currently, polymer-directed self-assembly of inorganic nanoparticles remains a challenging task. Typically, it has been achieved *via* a solvent switching method that is relatively tedious and limited by low nanoparticle concentration.[14–16] These observations suggest an intriguing question: can we utilize PISA to direct the self-assembly of inorganic nanoparticles *in situ* during the polymerization process and form well-defined nano-objects? To address this question, we designed a system based on bimodal polymer grafted nanoparticles. The procedure to synthesize such mixed brushes has been established using a sequential surface-initiated RAFT (SI-RAFT) polymerization strategy.[17] After the first SI-RAFT polymerization, active chain-end groups were removed by reacting with an excess of AIBN. Then, a second population of RAFT agent was grafted onto the particles surface and a second monomer was polymerized. The polymerizations were well-controlled, showing the common characteristics of living polymerization.

In this communication, we demonstrate the first case of surface-initiated polymerization-induced self-assembly by polymerizing benzyl methacrylate(BzMA) from SiO_2-*g*-(PHEMA, CPDB) nanoparticles which served as both chain transfer agent and stabilizer. Scheme 1A shows the synthetic route toward SiO_2-*g*-(PHEMA, CPDB) from bare 15 nm silica nanoparticles. Poly(2-hydroxyethyl methacrylate) (PHEMA) was selected as the first polymer brush since it is miscible with methanol, and has been previously reported as a stabilizing block for PISA.[18] The graft density of PHEMA was 0.1 ch per nm^2, as calculated from the characteristic RAFT UV-vis peak at 304 nm (see ESI† for details). The medium graft density secured enough polymer content to solubilize the silica nanoparticles, and yet left enough surface space for the growth of the second polymer population. Surface-initiated polymerization of HEMA was carried out in DMF at 65 °C, with molar ratio between species [RAFT] : [HEMA] : [AIBN] = 1 : 1000 : 0.15. After 5 hours, 19% conversion was achieved, corresponding to 190 repeat units and 24.7 kDa molecular weight (assuming 100% CTA efficiency). RAFT end groups were subsequently removed by reacting with 20 eq. AIBN.[17,19] The resulting PHEMA grafted nanoparticles were then treated with aminopropyldimethylethoxysilane and activated CPDB (see Scheme S1† for chemical structure) to immobilize a second RAFT agent. The second graft density was determined to be 0.15 ch per nm^2 based on UV analysis and TGA result (Fig. S1 and S2†).

The SiO_2-*g*-(PHEMA, CPDB) nanoparticles prepared in the previous steps were used to perform surface-initiated dis-

Department of Chemistry and Biochemistry, University of South Carolina, Columbia, SC, 29208, USA. E-mail: Benice.sc.edu

†Electronic supplementary information (ESI) available. See DOI: 10.1039/c6py01319h

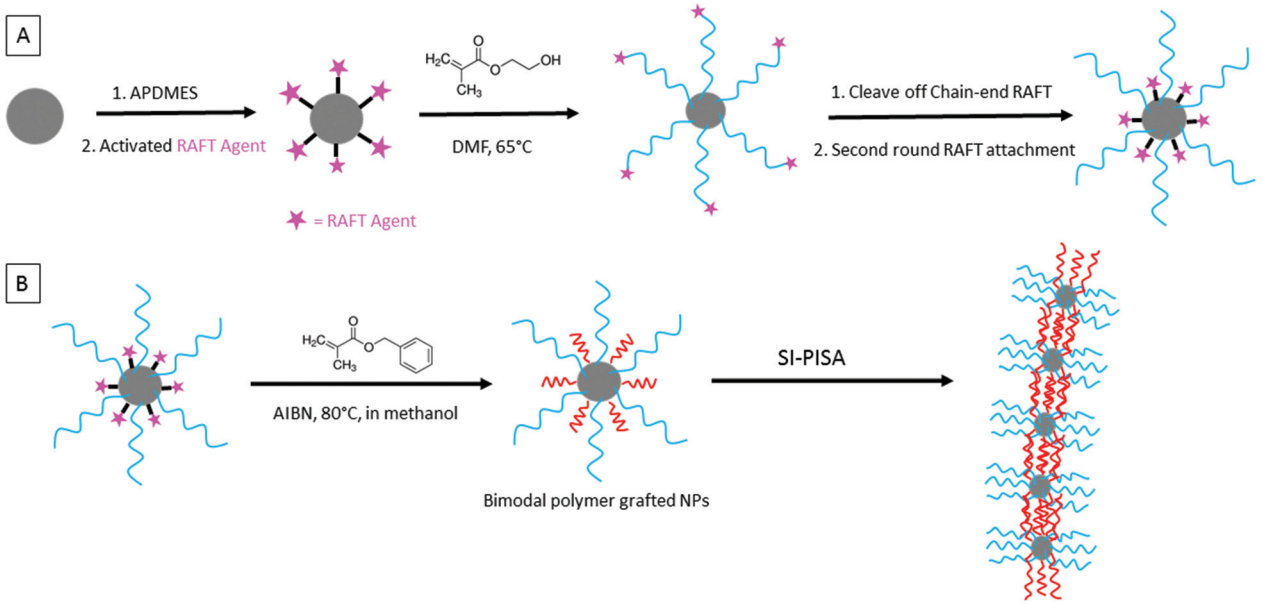

Scheme 1 (A) Synthesis of SiO_2-*g*-(PHEMA, CPDB) nanoparticles. (B) Surface-initiated RAFT dispersion polymerization of BzMA from SiO_2-*g*-(PHEMA, CPDB) nanoparticles in methanol.

persion RAFT polymerization of BzMA in methanol (Scheme 1B). The SiO_2-*g*-(PHEMA, CPDB) nanoparticles were well-dispersed in methanol to form a homogenous solution, to which BzMA, AIBN, and trioxane were added. The molar ratio between RAFT : BzMA : AIBN was set at 1 : 1200 : 0.15, with solid content 12% (w/w%). BzMA was selected since it has been widely used as a core forming material in alcoholic PISA systems and showed fast polymerization rate and high conversion.[20,21] The experimental design allows the surface PHEMA chains to solubilize each individual silica nanoparticle in methanol at the beginning of the polymerization. As the polymerization was initiated, PBzMA chains grew from the silica surface, forming (PHEMA, PBzMA) bimodal polymer-grafted nanoparticles. These bimodal nanoparticles were individually stable at the early stages when PBzMA chains were relatively short. However, with the continuous increase of insoluble PBzMA chain lengths, each particle became more and more solvophobic and beyond a certain point, self-assembly occurred to minimize the contact between PBzMA chains and the solvent.

Visual observation during polymerization indicated formation of assemblies (Fig. 1A). The polymerization solution was pink and transparent at 0 h, and gradually faded in color to become almost colorless, but still transparent at 1 h. Significant visual turbidity change began at 1.5 h, when a slightly turbid solution was formed. The turbidity increased with time and eventually formed a milky-white solution at 4.5 h. All the turbid solutions formed in the first 4.5 hours were homogenous and stable, with no macroscopic precipitation. However, samples after 5 hours were less stable with white precipitates forming on the walls of the reaction flask.

The initial pink color loss was quite interesting and worth noting, as it has not been observed in normal surface-initiated

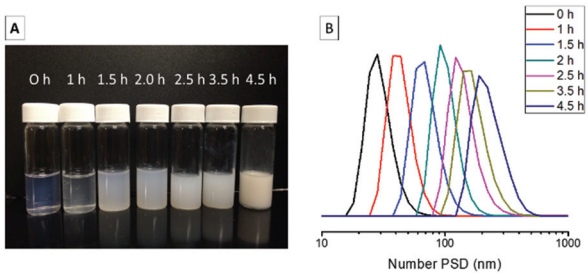

Fig. 1 (A) Optical digital photo of the surface-initiated RAFT polymerization at different times (B) DLS of polymerization solution at different times.

polymerization of methacrylates. We reason that the disappearance of pink color occurred at the onset of self-assembly, when the insoluble PBzMA chains collapsed and became wrapped into the core part of the assemblies. The surface-initiated RAFT polymerization was followed by ^{1}H NMR and gel permeation chromatography (GPC). Monomer conversion was calculated based on the ratio between the monomer vinyl peak at 5.6 ppm and the internal standard peak at 5.1 ppm (trioxane). GPC analysis was conducted by reacting polymer grafted nanoparticles with HF to cleave the chains from the silica surfaces, and then THF was used to selectively dissolve PBzMA. Details of reaction time, monomer conversions, GPC data, DLS data, and visual appearance are summarized in Table 1. Polymerization kinetics showed a linear relationship between $\ln([M]_0/[M])$ and time (Fig. 2A). The onset of turbidity at *ca.* 1.5 h corresponded to 49 repeat units of PBzMA, which is the critical degree of polymerization for phase separation in this case. The molecular weight of PBzMA increased linearly

Table 1 Summary of reaction time, monomer conversions, GPC data, DLS data, and visual appearance obtained for a series of SiO_2-*g*-(PHEMA, PBzMA) nanoparticles

Entry no.	Reaction time (h)	Conversion[a] (%)	Bimodal polymer composition[b]	M_n of PBzMA[c] (g mol^{-1})	M_w/M_n [d]	Number average size[e] (nm)	Visual appearance
153-0	0	—	$PHEMA_{190}$			28	Pink transparent solution
153-1	1	1.2	$PHEMA_{190}$ $PBzMA_{12}$	N/A	N/A	55	Very light pink transparent solution
153-2	1.5	4.9	$PHEMA_{190}$ $PBzMA_{49}$	13 000	1.12	71	Slightly turbid solution
153-3	2	5.8	$PHEMA_{190}$ $PBzMA_{58}$	14 500	1.16	100	Slightly turbid solution
153-4	2.5	7.0	$PHEMA_{190}$ $PBzMA_{70}$	16 000	1.16	142	Turbid solution
153-5	3.5	10.0	$PHEMA_{190}$ $PBzMA_{100}$	18 800	1.15	169	Turbid solution
153-6	4.5	12.1	$PHEMA_{190}$ $PBzMA_{121}$	21 500	1.13	225	Milky-white solution

[a] Determined by ^{1}H NMR spectroscopy. [b] Determined by ^{1}H NMR spectroscopy, assuming 100% RAFT agent efficiency. [c] Determined by size exclusion chromatography using PMMA as standard. [d] Determined by size exclusion chromatography. [e] Determined by dynamic light scattering. Number average size reported for all samples.

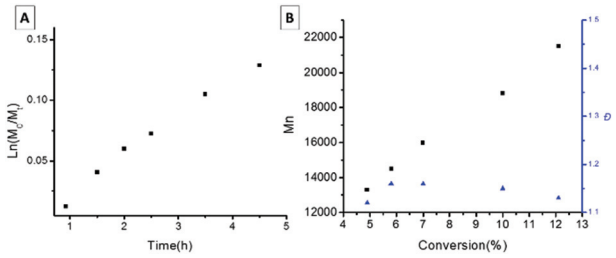

Fig. 2 (A) $\ln(M_0/M_t)$ *vs.* time plot for surface-initiated BzMA polymerization in methanol. (B) M_n and $Đ$ *vs.* monomer conversion plots for surface-initiated BzMA polymerization in methanol.

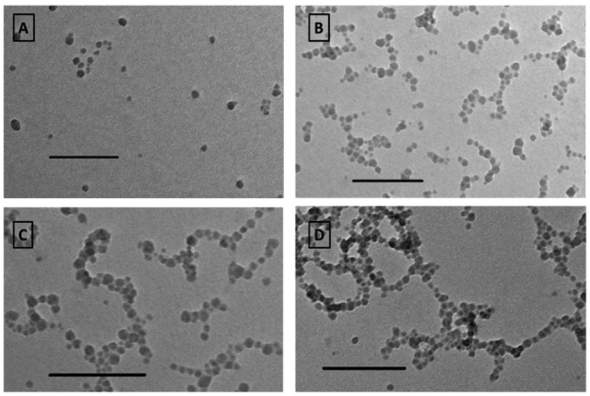

Fig. 3 TEM images of the morphologies formed at 0 h (A), 1.5 h (B), 2 h (C), and 4.5 h (D). All scale bars: 200 nm.

with conversion, with dispersity remaining below 1.2 (Fig. 2B). GPC traces showed a gradual shift toward higher molecular weights as the polymerization proceeded (Fig. S3†). All the results suggested that the surface-initiated RAFT dispersion polymerization of PBzMA was well controlled with PHEMA grafted nanoparticles as stabilizer.

DLS studies indicated an increase in the hydrodynamic size of nanoparticles with reaction time, which is consistent with the turbidity change observed during polymerization. Number average sizes were reported to offer comparison with the size of aggregates observed with TEM.[11] The solution before reaction (0 h) had a number-average diameter of 28 nm, which corresponds to individually dispersed PHEMA grafted nanoparticles. At 1.5 h, when the initial turbidity change could be visually observed, the average particle size increased to 71 nm, indicating a slight degree of agglomeration between nanoparticles. The mean particle diameter grew progressively with polymerization time, and reached 225 nm at 4.5 hour, when a milky-white solution was formed.

In order to investigate the morphology of nanoparticle assemblies, TEM was used to follow the polymerization and representative images are shown in Fig. 3. Fig. 3A showed that particles were individually dispersed in methanol before reaction. At 1.5 h, particles began to connect with each other and formed mostly one-dimensional short strings composed of several nanoparticles (Fig. 3B). As the polymerization continued, the strings became longer and formed branched structures (Fig. 3C). At 4.5 h, highly branched string structures were formed, accompanied with higher degree of aggregation at junction points. Samples after 5 h formed cross-linked nanoparticle networks (Fig. S7†) that eventually precipitated from solution (see ESI† for more TEM images).

The basis for the self-assembly process is explained in Scheme 2. When the PBzMA chains became sufficiently long, the mixed polymer brushes will first phase separate (due to polymer–polymer immiscibility) by chain-stretching and rearranging to form surface PHEMA domains and surface PBzMA domains. Then, the PBzMA domains between nanoparticles will aggregate (due to polymer–solvent immiscibility) with each other to form nanoparticle pairs. The closely associ-

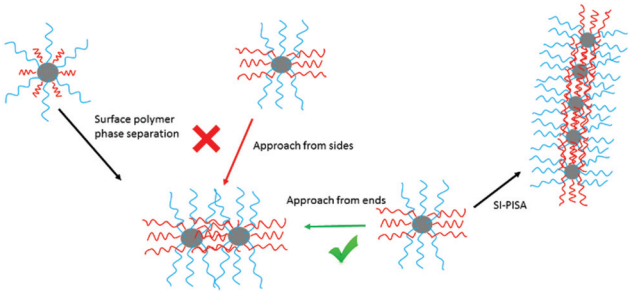

Scheme 2 Proposed mechanism of SI-PISA of silica nanoparticles into strings.

ated nanoparticle pairs lead to a higher PHEMA polymer density around the centre than the poles of nanoparticle pairs. As a result, the following nanoparticles could only approach from the ends, forming nanoparticle strings. This self-assembly mechanism is supported by TEM images at high magnification (Fig. S8†). It is clear that the nanoparticles were not in direct contact with each other. Instead, there was a 5–8 nm gap between each nanoparticle pair, which represents the collapsed PBzMA domain.

It is worth noting that the self-assembly mechanism of these bimodal polymer grafted nanoparticles is different from most of the polymer-directed 1D colloidal assemblies reported previously, where sparsely grafted homopolymers[22] or block copolymers[23,24] were used to direct the anisotropic assembly. The anisotropy, in this case, originated from the phase separation of immiscible polymer brushes and guided the *in situ* formation of 1D assemblies without the need of any post-polymerization process.

Conclusions

In summary, we described the first case of surface-initiated polymerization-induced self-assembly of nanoparticles by polymerizing benzyl methacrylate (BzMA) from SiO_2-*g*-(PHEMA, CPDB) nanoparticles which served as both chain transfer agent and stabilizer. With the increase in chain length of the PBzMA brush, the nanoparticles self-assembled into a variety of 1-D structures including short strings, branched long strings, and highly branched string networks. All the assembled hybrid structures were very stable and could be produced in one step at high nanoparticle concentration. We believe that this SI-PISA strategy is a facile and efficient way of preparing hybrid assemblies. Furthermore, by adjusting the chain length and graft density of the brushes, this method could be extended to make various shapes of hybrid assemblies, that may find broad applications in nanotechnology.

Notes and references

1 G. Zheng and C. Pan, *Macromolecules*, 2006, **39**, 95–102.
2 W.-M. Wan and C.-Y. Pan, *Polym. Chem.*, 2010, **1**, 1475–1484.
3 B. Charleux, G. Delaittre, J. Rieger and F. D'Agosto, *Macromolecules*, 2012, **45**, 6753–6765.
4 N. J. Warren and S. P. Armes, *J. Am. Chem. Soc.*, 2014, **136**, 10174–10185.
5 A. Blanazs, J. Madsen, G. Battaglia, A. J. Ryan and S. P. Armes, *J. Am. Chem. Soc.*, 2011, **133**, 16581–16587.
6 G. Delaittre and B. Charleux, *Macromolecules*, 2008, **41**, 2361–2367.
7 W.-M. Wan and C.-Y. Pan, *Macromolecules*, 2007, **40**, 8897–8905.
8 S. L. Canning, G. N. Smith and S. P. Armes, *Macromolecules*, 2016, **49**, 1985–2001.
9 H. Zhou, C. Liu, C. Gao, Y. Qu, K. Shi and W. Zhang, *J. Polym. Sci., Part A: Polym. Chem.*, 2016, **54**, 1517–1525.
10 M. J. Derry, L. A. Fielding and S. P. Armes, *Prog. Polym. Sci.*, 2016, **52**, 1–18.
11 R. Bleach, B. Karagoz, S. M. Prakash, T. P. Davis and C. Boyer, *ACS Macro Lett.*, 2014, **3**, 591–596.
12 J. Tan, H. Sun, M. Yu, B. S. Sumerlin and L. Zhang, *ACS Macro Lett.*, 2015, **4**, 1249–1253.
13 C. J. Mable, R. R. Gibson, S. Prevost, B. E. McKenzie, O. O. Mykhaylyk and S. P. Armes, *J. Am. Chem. Soc.*, 2015, **137**, 16098–16108.
14 J. He, Y. Liu, T. Babu, Z. Wei and Z. Nie, *J. Am. Chem. Soc.*, 2012, **134**, 11342–11345.
15 J. Song, L. Cheng, A. Liu, J. Yin, M. Kuang and H. Duan, *J. Am. Chem. Soc.*, 2011, **133**, 10760–10763.
16 J. Wang, W. Li and J. Zhu, *Polymer*, 2014, **55**, 1079–1096.
17 A. Rungta, B. Natarajan, T. Neely, D. Dukes, L. S. Schadler and B. C. Benicewicz, *Macromolecules*, 2012, **45**, 9303–9311.
18 D. Zehm, L. P. D. Ratcliffe and S. P. Armes, *Macromolecules*, 2013, **46**, 128–139.
19 S. Perrier, P. Takolpuckdee and C. A. Mars, *Macromolecules*, 2005, **38**, 2033–2036.
20 M. J. Derry, L. A. Fielding and S. P. Armes, *Polym. Chem.*, 2015, **6**, 3054–3062.
21 J. Yeow, J. Xu and C. Boyer, *ACS Macro Lett.*, 2015, **4**, 984–990.
22 M. S. Nikolic, C. Olsson, A. Salcher, A. Kornowski, A. Rank, R. Schubert, A. Frömsdorf, H. Weller and S. Förster, *Angew. Chem., Int. Ed.*, 2009, **48**, 2752–2754.
23 Y. Liu, J. He, K. Yang, C. Yi, Y. Liu, L. Nie, N. M. Khashab, X. Chen and Z. Nie, *Angew. Chem., Int. Ed.*, 2015, **54**, 15916–15916.
24 Y. Kang, K. J. Erickson and T. A. Taton, *J. Am. Chem. Soc.*, 2005, **127**, 13800–13801.